International Journal of Minerals, Metallurgy and Materials
Volume 25, Number 7, July 2018, Page 744
https://doi.org/10.1007/s12613-018-1622-7

Preparation of ferronickel from nickel laterite via coal-based reduction followed by magnetic separation

*Lun-wei Wang*1), *Xue-ming Lü*1), *Mei Liu*2), *Zhi-xiong You*1), *Xue-wei Lü*1), *and Chen-guang Bai*1)

1) College of Materials Science and Engineering, Chongqing University, Chongqing 400044, China
2) Engineer of CISDI Thermal & Environmental Engineering Co., Ltd., Chongqing 401122, China

(Received: 18 October 2017; revised: 12 January 2018; accepted: 30 January 2018)

Abstract: The sticking phenomenon between molten slag and refractory is one of the crucial problems when preparing ferronickel from laterite ore using rotary hearth furnace or rotary kiln processes. This study aims to ameliorate sticking problems by using silicon dioxide (SiO_2) to adjust the melting degree of the briquette during reduction roasting. Thermodynamic analysis indicates that the melting temperature of the slag gradually increases with an increase in the SiO_2 proportion ($SiO_2/(SiO_2 + Al_2O_3 + MgO)$ mass ratio). Experimental validations also prove that the briquette retains its original shape when the SiO_2 proportion is greater than 75wt%, and sticking problems are avoided during reduction. A ferronickel product with 8.33wt% Ni and 84.71wt% Fe was prepared via reductive roasting at 1500°C for 90 min with a SiO_2 proportion of 75wt% and a C/O molar ratio of 1.0 followed by dry magnetic separation; the corresponding recoveries of Ni and Fe reached 75.70% and 77.97%, respectively. The microstructure and phase transformation of reduced briquette reveals that the aggregation and growth of ferronickel particles were not significantly affected after adding SiO_2 to the reduction process.

Keywords: nickel laterite; carbothermal reduction; ferronickel; magnetic separation

1. Introduction

Nickel is an important strategic metal that has been widely applied as an alloying component in the production of stainless steels and special steels [1]. In recent years, the world annual demand for nickel (in the form of pure nickel metal or as a ferronickel alloy with a variable iron grade) has increased tremendously, due to soaring stainless steel production [2–5]. Nickel is mainly extracted from sulfide and laterite type nickel ores, which account for approximately 36wt% and 64wt% of worldwide nickel reserves, respectively [6–9]. With the gradual exhaustion of sulfide ores and high-grade nickel resources, considerable attention is being focused on recovering nickel from low-grade nickel laterite ores [10].

Nickel in nickeliferous laterite ore always exists as an isomorphous substitution for iron or magnesium in the lattice of iron oxide or silicate minerals. Physical methods have proven to be inefficient for use in recovering nickel, due to its complex mineralogy. In addition, hydrometallurgical processes, including high pressure acid leaching (HPAL) [11], reduction roasting-ammonia leaching (Caron process), and atmospheric leaching (AL), are also considered to have low efficiencies; they provide low nickel recovery and produce iron-bearing waste [12].

To date, a pyrometallurgical method known as the rotary kiln–electric furnace (RKEF) process [13–14], has been applied to produce ferronickel from nickel laterite ore. The RKEF process involves calcination and pre-reduction at 800–1000°C for 4–6 h in a rotary kiln, followed by semlting at 1550–1600°C for 2–3 h in an electric arc furnace, to separate ferronickel from slag. The process is characterized by its intensive energy consumption [15]. Preparation of ferronickel alloy via direct reduction in the rotary kiln (RK) followed by physical separation (magnetic/ gravity) has also been employed by the Nippon Yakin Kogyo Co., Ltd. of Japan [16]. Although the ferronickel materials obtained from physical separation can be directly used to manufacture

---

Corresponding authors: Zhi-xiong You, E-mail: youzx@cqu.edu.cn; Xue-wei Lü, E-mail: lvxuewei@163.com

stainless steels, this process requires a temperature of 1250–1400°C during reduction to partially melt the slag and to obtain a desirable growth of ferronickel granules. The major problems with this technology are the formation of rings inside the RK and corrosion of the refractory [17]. In this respect, an alternative method of direct reduction has been investigated using relatively lower roasting temperatures (1000–1300°C) followed by wet magnetic separation. Ma *et al.* [18] systematically investigated the process of ferronickel production from nickel laterite (Ni: 0.80wt%, TFe: 10.90wt%) using non-molten state reduction, and a ferronickel concentrate with a Ni grade of 4.4% and nickel recovery of 9.4% was obtained by reduction roasting at 1250°C for 100 min in the absence of additives followed by wet magnetic separation. Nevertheless, most of the studies were still in the laboratory. In addition, additives of $NaSO_4$, CaF, and CaO are always used during reductive roasting to improve the growth of ferronickel granules, which causes heavy environment pollution and equipment corrosion [18–22].

In the last few decades, huge advances have been made in the application of non-blast-furnace ironmaking processes to rotary hearth furnace (RHF) technology [23–24]; these processes can be applied in the process of ferroalloy production. However, direct reduction in a RK or RHF causes sticking between the molten slag and refractory, and the life of the refractory and its stability during discharging are severely affected when it is eroded by slag.

To avoid the use of corrosive additives, and to relieve sticking problems during reductive roasting, silicon dioxide (SiO_2) is used in this study to increase the melting temperature of reduced briquette. After achieving the carbothermal reduction of nickel laterite with added silicon dioxide, the use of dry magnetic separation is then investigated, and the effect of the SiO_2 proportion ($SiO_2/(SiO_2 + Al_2O_3 + MgO)$ mass ratio) and reduction parameters on ferronickel preparation are also researched. Furthermore, X-ray diffraction (XRD) and scanning electron microscope (SEM) are used to observe the phase transformation and microstructure of the reduced product, respectively.

2. Experimental

2.1. Raw materials

The nickel laterite ore used in this study was obtained from the Philippines. The main chemical composition of the raw material is shown in Table 1. The Ni grade and total iron grade (TFe) were 1.81% and 17.87%, respectively, and it can be observed that the sample has a high grade of silica, magnesia, alumina, and water (includes: free water, crystal water, and hydroxyl groups). A mineralogical analysis of the sample was conducted using X-ray diffraction (XRD), and the results in Fig. 1 indicate that the laterite ore is mainly composed of lizardite ($(Mg,Al)_3(Si,Fe)_2O_5(OH)_4$, $Mg_3Si_2O_5(OH)_4$), hematite (Fe_2O_3), and gismondine ($CaAl_2Si_2O_8(H_2O)_4$). The grade of nickel is low, which is mostly associated with lizardite and maghemite as isomorphous substitution for magnesium and iron.

Table 1. Main chemical composition of nickel laterite ore wt%

Ni	TFe	Cr_2O_3	SiO_2	Al_2O_3	CaO	MgO	P	S	Moisture
1.81	17.87	0.51	34.97	4.75	1.54	13.5	0.005	0.064	17.35

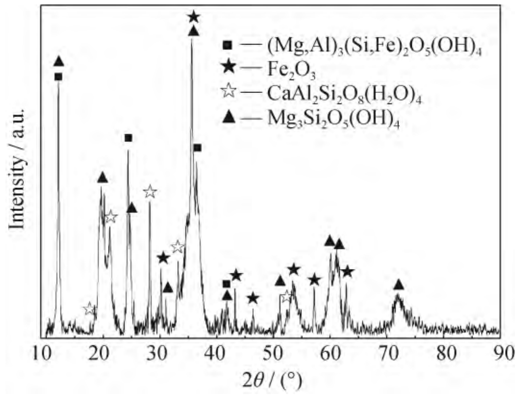

Fig. 1. XRD pattern of nickel laterite.

Pulverized coke with particles sizes smaller than 1 mm was used as the reducing agent, and an industry analysis of the coke is presented in Table 2. Analytical reagent (AR) grade silicon dioxide was used to adjust the melting degree during reduction roasting.

Table 2. Industry analysis of pulverized coke wt%

Fixed carbon	Ash	Volatile	P	S
76.11	10.71	13.15	0.08	0.43

2.2. Methods

The nickel laterite was dried at 120°C for 2 h in an oven, ground to 80wt% of the particles smaller than 0.074 mm, mixed to homogeneity with pulverized coke and powdery silicon dioxide, and then briquetted into a cylinder (ϕ30 mm × 10 mm) using a powder tablet press machine at a pressure of 15 MPa (no binder was used in the briquetting process).

The reduction process was conducted in a resistance furnace, in which the roasting temperature was controlled within ±2°C. A schematic diagram of the experimental apparatus is presented in Fig. 2. When the furnace was pre-heated to the required temperature, argon was passed through the furnace to expel air. To load the briquettes, a graphite crucible was introduced into a protective crucible in the hot zone of the furnace. After roasting for the desired time period under an argon atmosphere, the crucible was removed from the furnace and quenched rapidly to room temperature. Finally, the reduced sample was manually crushed to particle sizes of less than 3 mm and prepared for dry magnetic separation. A mineralogical observation and chemical composition analysis was also conducted.

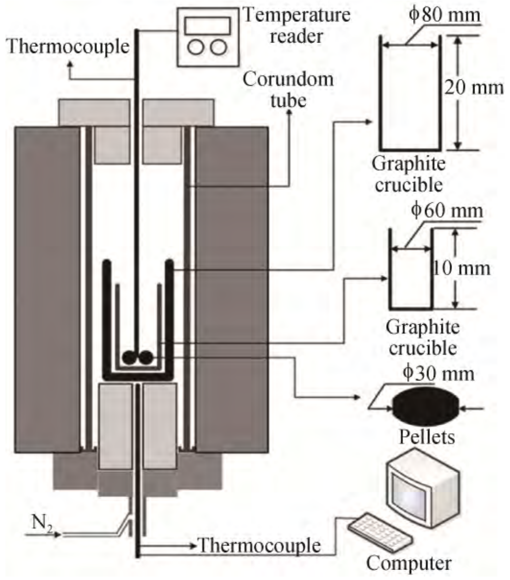

Fig. 2. Schematic diagram of reduction furnace.

2.3. Evaluation indexes

The amount of Ni and Fe recovered in each sample was calculated according to formulas (1) and (2), respectively,

$$\eta_{\mathrm{Ni}}=\frac{MX_{\mathrm{Ni}}}{M_0X_{\mathrm{Ni}}^0}\times 100\% \tag{1}$$

$$\eta_{\mathrm{Fe}}=\frac{MX_{\mathrm{Fe}}}{M_0X_{\mathrm{Fe}}^0}\times 100\% \tag{2}$$

where η_{Ni} is the recovery of Ni, %; η_{Fe} is the recovery of Fe, %; M is the mass of magnetic fraction, g; X_{Ni} is the grade of Ni in the magnetic fraction, %; X_{Fe} is the grade of Fe in the magnetic fraction, %; M_0 is the mass of raw laterite nickel in reduction sample, g; X_{Ni}^0 is the grade of Ni in the nickel laterite; and X_{Fe}^0 is the grade of Fe in the nickel laterite.

3. Thermodynamic analysis

As previously mentioned, the sticking phenomenon between reduced briquettes and refractory is one of the crucial problems inherent in RHF and RK processes. To understand the effect of SiO_2 on the melting temperature of the slag during reduction, a SiO_2–MgO–FeO–Al_2O_3–CaO pseudo-ternary phase diagram was calculated using the Phase Diagram of FactSage 6.2 in the range of 1350–1600°C. The FToxide database was used in the calculation process and all solutions of the database were considered. Only the liquid slag phase was plotted in the pseudo-ternary phase diagram, and the results are shown in Fig. 3. The mass ratios of CaO/(SiO_2 + Al_2O_3 + MgO) and Al_2O_3/(SiO_2 + Al_2O_3 + MgO) were fixed at 0.03 and 0.08, respectively, according to the chemical composition of the raw nickel laterite ore (shown in Table 1). Line 1 in Fig. 3 represents the original components of the laterite ore (the SiO_2 proportion equals 65wt%). The results indicate that the melting temperature of the slag occurred at approximately 1400°C; therefore, the briquette melted when reduced at about 1400°C. However, by increasing the SiO_2 proportion from 65wt% to 80wt%, the melting temperature of slag gradually increased to approximately 1650°C. It is thus considered that the melting degree of slag can be controlled by adjusting the SiO_2 grade, and the sticking phenomenon is also inhibited.

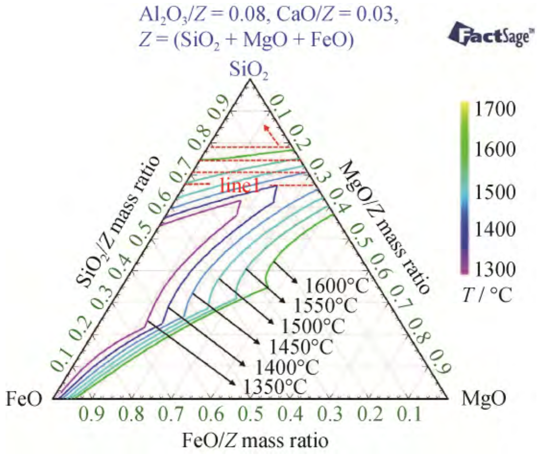

Fig. 3. Liquid phase diagram of SiO_2–MgO–FeO–Al_2O_3–CaO system.

4. Results and discussion

4.1. Effect of the SiO_2 proportion

The effect of the SiO_2 proportion on reduction was investigated by maintaining the reduction temperature at 1500°C and using a reduction time of 60 min with a C/O molar ratio of 1.2. The morphology and magnetic separation results for reduced briquettes are shown in Figs. 4 and 5, respectively.

As shown in Fig. 4, the cylindric briquettes changed to spherical pellets with SiO_2 proportions of 65wt% and 70wt%; this result is mainly attributed to the melting of slag during reduction. As previously mentioned, melted slag sticks to the crucible after cooling; however, the sticking phenomenon between the molten slag and refractory material does not occur during the reduction process. The life of the refractory and the stability during discharging is seriously affected when the refractory is eroded by the slag, but when the proportion of SiO_2 is increased to 75wt%, the briquette retains its original morphology and the sticking problem is inhibited.

The magnetic separation results of reduced laterite ore with no addition of SiO_2 (shown in Fig. 5) indicate that the Ni and Fe grades of the magnetic fraction were 6.63% and 80.09%, respectively. As the SiO_2 proportion was increased to 75wt%, there were evident decreases in the grades of Ni and Fe (2.13% and 26.14%), and their recoveries also correspondingly decreased. Although the grades and recoveries of Ni and Fe with no addition of SiO_2 are desirable prior to adjustment of the SiO_2 grade, as previously mentioned, both ferronickel particles and molten slag adhere to the bottom of the crucible and it is difficult to separate them from it.

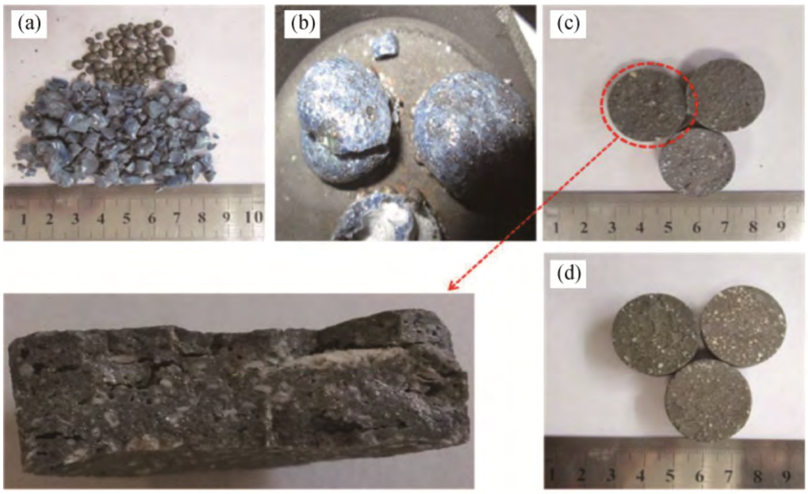

Fig. 4. Samples after reduction at 1500°C with different SiO_2 proportions: (a) 65wt%; (b) 70wt%; (c) 75wt%; (d) 80wt%.

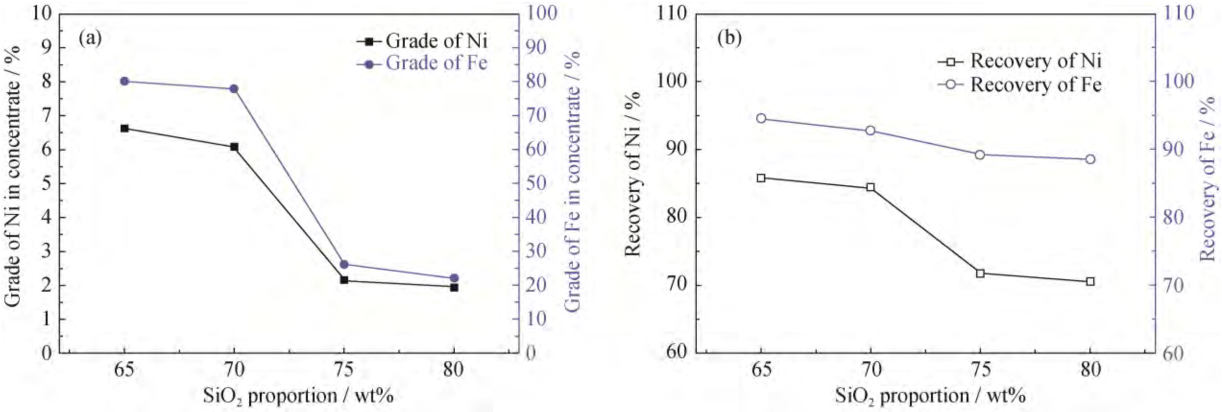

Fig. 5. Effect of SiO_2 proportion on Ni and Fe grades (a) and recoveries (b) (reduction temperature of 1500°C, reduction time of 60 min, and C/O molar ratio of 1.2).

In an attempt to explain the above phenomenon, theoretical liquid phase generation with different SiO_2 proportions was calculated using the Equilib module of FactSage 6.2. In the calculation process, the database of Fact53 was used, the reactants were SiO_2, Al_2O_3, MgO, CaO, and Fe_2O_3, and the mass ratio of the reactants was based on the chemical composition of the raw nickel laterite ore shown in Table 1. In addition, the reductant was carbon and the C/O molar ratio was fixed at 1.2. When the reactions reached equilibrium in the range of 1000–1600°C, the theoretical liquid phase amount was calculated. As shown in Fig. 6, the SiO_2 proportion in raw laterite ore was 65wt% and the theoretical liquid phase amount was 96wt% at 1500°C. By adjusting the SiO_2 proportion from 65wt% to 70wt%, the theoretical liquid phase amount decreased slightly from 96wt% to 94wt% at 1500°C. However, this amount was decreased to 78wt% when the SiO_2 proportion was increased to 75wt%. As a result, the samples remained cylindrical and did not adhere to the crucible after reduction. Although a decrease in liquid phase generation is disadvantageous to the aggregation and the growth of ferronickel particles, it is considered to be more beneficial for smoothly separating the briquettes from the crucible after reduction in the RHF process. Therefore, a SiO_2 proportion of 75wt% was used in subsequent experiments.

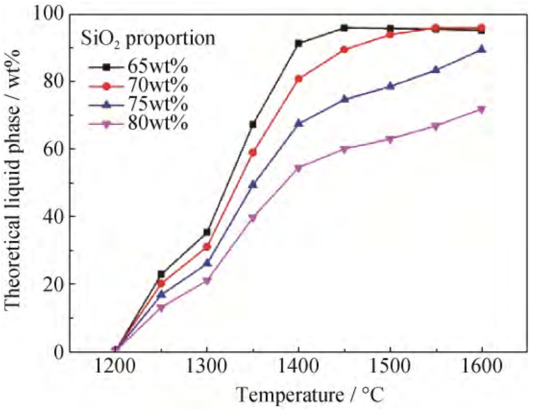

Fig. 6. Theoretical liquid phase generation with different SiO_2 proportions.

4.2. Effect of reduction temperature

The effect of reduction temperature on the recoveries of Ni and Fe was studied under the following conditions: the SiO_2 proportion of 75wt%, reduction time of 60 min, and C/O molar ratio of 1.2. The results, which are plotted in Fig. 7(a), indicate that both the Ni and Fe grades reached maximum values when the reduction temperature was increased to 1450°C and then gradually decreased. This is mainly because that the silicon and chromium were reduced into alloys with the increase of temperature, thus resulting in the Ni and Fe in the concentrate was diluted. As the temperature increased from 1400°C to 1500°C, the recovery of Ni increased from 37.29% to 71.69%, and Fe recovery increased from 49.40t% to 89.25%. Therefore, an increase in the reduction temperature enhanced nickel and iron oxide reduction and more of the liquid phase was formed, thereby intensifying the aggregation and growth of the ferronickel particles. It is thus evident that increasing the reduction temperature is an effective way of increasing the enrichment efficiency of nickel. Hence, a reduction temperature of 1500°C is adequate for the preparation of ferronickel.

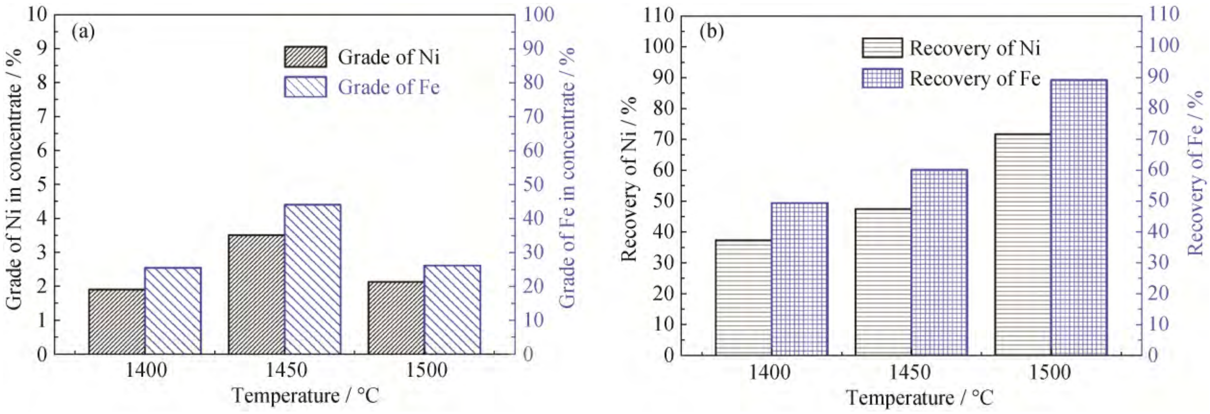

Fig. 7. Effect of temperature on Ni and Fe grades (a) and recoveries (b) (SiO_2 proportion of 75wt%, reduction time of 60 min, and C/O molar ratio of 1.2).

4.3. Effect of reduction time

By fixing the SiO_2 proportion at 75wt%, the reduction temperature at 1500°C, and C/O molar ratio at 1.2, the effect of the reduction time on the grades and recoveries of Ni and Fe was examined, as shown in Fig. 8. It can be observed from Fig. 8(a) that when the reduction time was prolonged to 90 min, the grades of Ni and Fe in the magnetic fraction were distinctly improved to 5.63% and 71.82%, respectively; however, the grades decreased slightly with a further increase in the reduction time to 120 min. This is mainly attributed to the reduction of a greater amount of SiO_2 to elemental silicon, and the generated silicon combining with metallic iron and turning into the magnetic fraction. In addition, a slight decrease in Ni and Fe recoveries was observed when the reduction time was varied from 60 to 120 min, as shown in Fig. 8(b). This is mainly attributed to an insufficient reduction atmosphere at the end of the reduction process, which resulted in reoxidation of the reduced metallic nickel and iron. These results show that the most suitable reduction time is 90 min.

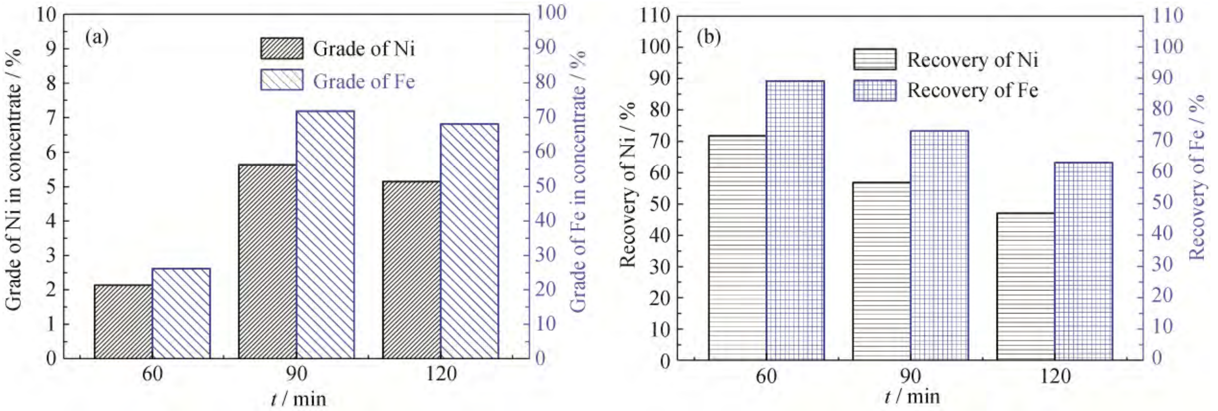

Fig. 8. Effect of time on Ni and Fe grades (a) and recoveries (b) (SiO_2 proportion of 75%, reduction temperature of 1500°C, and C/O molar ratio of 1.2).

4.4. Effect of C/O molar ratio

With the aim of optimizing the C/O molar ratio for preparing ferronickel, experiments were conducted with C/O molar ratios ranging from 0.8 to 1.2. The SiO_2 proportion, reduction time, and temperature were maintained at 75wt%, 90 min, and 1500°C, respectively. The results presented in Fig. 9(a) show a slight decrease in the grades of Ni and Fe from 8.82% to 8.33% and 86.94% to 84.71%, respectively, with an increase in the C/O molar ratio from 0.8 to 1.0, but then an evident decrease to 5.63% and 71.82% with a C/O molar ratio of 1.2. These results are mainly attributed to the carburization phenomenon and reduction of SiO_2 when more carbon is added to the reduction process. The recoveries of both Ni and Fe increased and then decreased with an increase in the C/O molar ratio from 0.8 to 1.2. The corresponding recoveries of Ni and Fe reached 75.70% and 77.97%, respectively, when the C/O molar ratio is 1.0.

The above analysis suggests that a lower C/O molar ratio is favorable for increasing the Ni grade in the magnetic fraction. By adding an insufficient amount of reducing agent, it is actually feasible to thoroughly reduce nickel oxide while maintaining reduction of part of the iron oxide, which improves the nickel grade in the ferronickel material. The insufficient reduction of iron oxides allows more wustite (FeO) to enter the slag, which then decreases the melting point of slag; this is beneficial for aggregation and growth of the ferronickel particles. The SiO_2–MgO–FeO–Al_2O_3–CaO pseudo-ternary phase diagram is shown in Fig. 3, and it can be seen that the liquid slag phase shifts to a low temperature region along with an increase in the FeO grade. A higher C/O molar ratio allows more iron oxide to be reduced; this results in a decrease in the liquid slag and makes metal accumulation difficult. It is thus considered that a C/O molar ratio of 0.8–1.0 is sufficient for recovering Ni and Fe.

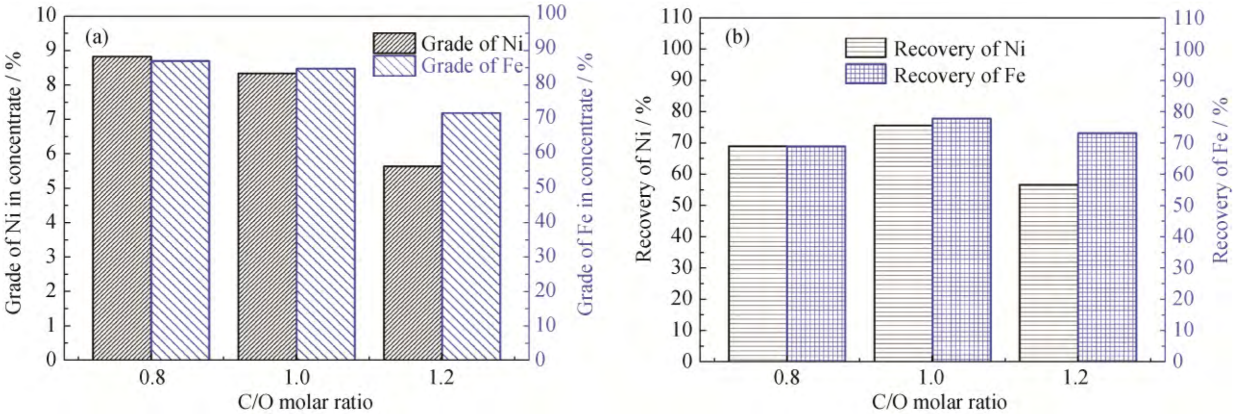

Fig. 9. Effect of C/O molar ratio on Ni and Fe grades (a) and recoveries (b) (SiO_2 proportion of 75wt%, reduction time of 90 min, and reduction temperature of 1500°C).

4.5. Growing character and phase transformation during reduction

The microstructures of reduced briquettes were studied using scanning electron microscope–energy dispersive spectrometer (SEM–EDS) analysis to characterize the growing character of ferronickel particles during reduction roasting. The results obtained under conditions of the SiO_2 proportion of 75wt%, reduction temperature of 1500°C, reduction time of 90 min, and a C/O molar ratio of 1.0 are shown in Fig. 10, where it is evident that the ferronickel particle (point 1) is well aggregated and that it grew to a size larger than 1 mm. Only a very small number of metal particles can be observed in the SEM images, which is favorable for subsequent magnetic separation. The main chemical composition of ferronickel particles is Fe, Ni, Si, Cr, and C, as shown in Fig. 10(b); silicon mainly exists in the form of elemental silicon, which is in accordance with a previous discussion. Gangue minerals (bearing Si, Mg, and Al) are detected in the EDS results of slag (point 2, Fig. 10(c)). From the surface scanning images (Figs. 10(d)–10(g)), iron and nickel are seen to be distributed almost uniformly in the same particle, which also indicates that iron and nickel oxides are reduced to a metallic state. In addition, metallic iron and nickel aggregated together and Mg and Si were turned into slag.

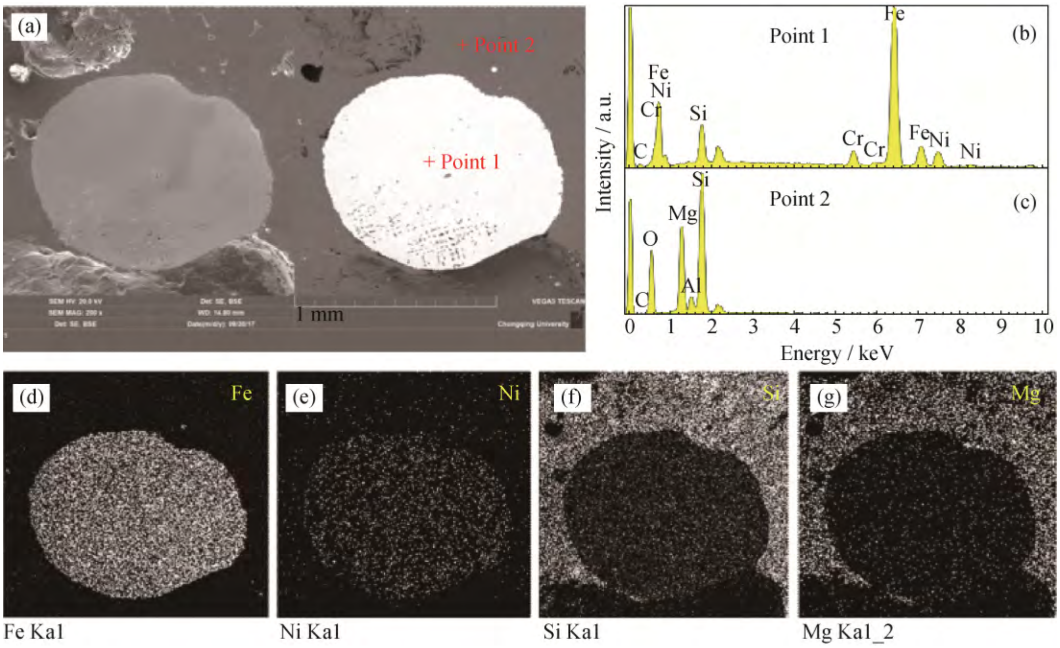

Fig. 10. SEM image (a) and EDS analyses (b–g) of reduction roasting production.

To determine the phase transformation during reduction after adjusting the SiO_2 proportion, XRD analysis was performed to determine the phase compositions of magnetic and nonmagnetic fractions. The XRD patterns are compared in Fig. 11, indicating that ferronickel (Fe,Ni) and ferronickel bearing Cr and C are present in the magnetic fraction.

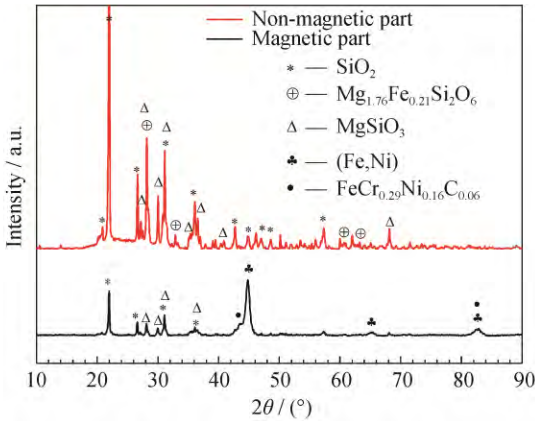

Fig. 11. XRD patterns of non-magnetic and magnetic parts.

However, small amounts of $MgSiO_3$ and SiO_2 also mingled with the ferronickel particles and were turned into magnetic material. The main phases in the XRD results of nonmagnetic material include olivine ($MgSiO_3$, $Mg_{1.76}Fe_{0.21}Si_2O_6$) and dissociative silica (SiO_2).

5. Conclusions

This study aimed to develop a method for avoiding the sticking problem between briquette and refractory during reduction roasting. In this respect, silicon dioxide (SiO_2) was used to adjust the melting degree of the briquette, and the main conclusions are presented as follows.

(1) Theoretical calculations show that the melting temperature of slag can be increased by adding SiO_2 in laterite ore. Experimental validations prove that the briquette remained cylindric when the SiO_2 proportion (SiO_2/(SiO_2 + Al_2O_3 + MgO) mass ratio) was greater than 75wt%, and that sticking problems were avoided during reduction.

(2) A ferronickel product with 8.33% Ni and 84.71t% Fe

was prepared via reductive roasting at 1500°C for 90 min with a SiO_2 proportion of 75wt% and C/O molar ratio of 1.0 followed by dry magnetic separation. The corresponding recoveries of Ni and Fe reached 75.70wt% and 77.97wt%, respectively.

Acknowledgements

The authors express gratitude to the National Natural Science Foundation of China (No. 51234010) and the Fundamental Research Funds for Central Universities (No. 106112017CDJXY130001) for the financial support provided for this research.

References

[1] M.O. Speidel, Nitrogen containing austenitic stainless steels, *Mat-wiss. u. Werkstoiftech.*, 37(2006), No. 10, p. 875.

[2] M. Liu, X.W. Lv, E.G. Guo, P. Chen, and Q.G. Yuan, Novel process of ferronickel nugget production from nickel laterite by semi-molten state reduction, *ISIJ Int.*, 54(2014), No. 8, p. 1749.

[3] G.M. Mudd, Global trends and environmental issues in nickel mining: Sulfides versus laterites, *Ore Geol. Rev.*, 38(2010), No. 1-2, p. 9.

[4] M.J. Rao, G.H. Li, T. Jiang, J. Luo, Y.B. Zhang, and X.H. Fan, Carbothermic reduction of nickeliferous laterite ores for nickel pig iron production in China: A review, *JOM*, 65(2013), No. 11, p. 1573.

[5] D.Q. Zhu, Y. Cui, K. Vining, S. Hapugoda, J. Douglas, J. Pan, and G.L. Zheng, Upgrading low nickel grade laterite ores using selective reduction followed by magnetic separation, *Int. J. Miner. Process.*, 106-109(2012), p. 1.

[6] A.D. Dalvi, W.G. Bacon, and R.C. Osborne, The past and the future of nickel laterites, [in] *PDAC 2004 International Convention, Trade Show and Investors Exhange*, Toronto, 2004, p. 1.

[7] X.W. Lv, C.G. Bai, S.P. He, and Q.Y. Huang, Mineral change of philippine and indonesia nickel lateritic ore during sintering and mineralogy of their sinter, *ISIJ Int.*, 50(2010), No. 3, p. 380.

[8] C. Pan, C.G. Bai, X.W. Lv, M.L. Hu, and T. Hu, Gaseous reduction of pellets of laterite ore containing carbon, *Metal. Int.*, 16(2011), No. 1, p. 5.

[9] X.M. Lv, X.W. Lv, L.W. Wang, J. Qiu, and M. Liu, Viscosity and structure evolution of the SiO_2–MgO–FeO–CaO–Al_2O_3 slag in ferronickel smelting process from laterite, *J. Min. Metall. Sect. B*, 53(2017), No. 2, p. 147.

[10] X.M. Lv, X.W. Lv, L.W. Wang, and J. Qiu. Thermal analysis kinetics of the solid-state reduction of nickel laterite ores by carbon, [in] *8th International Symposium on High-Temperature Metallurgical Processing*, San Diego, 2017, p. 147.

[11] W. Luo, Q.M. Feng, L.M. Ou, G.F. Zhang, and Y.P. Lu, Fast dissolution of nickel from a lizardite-rich saprolitic laterite by sulphuric acid at atmospheric pressure, *Hydrometallurgy*, 96(2009), No. 1-2, p. 171.

[12] G.W. Miller and H.Y. Liu. *Process for Recovery of Nickel and Cobalt by Heap Leaching of Low Grade Nickel or Cobalt Containing Material*, US patent, Appl. 04737564.7, 2010.

[13] R.A. Bergman, Nickel production from low-iron laterite ores: Process descriptions, *CIM Bull.*, 96(2003), No. 1072, p. 127.

[14] T. Norgate and S. Jahanshahi, Low grade ores — Smelt, leach or concentrate? *Miner. Eng.*, 23(2010), No. 2, p. 65.

[15] E.N. Zevgolis, C. Zografidis, T. Perraki, and E. Devlin, Phase transformations of nickeliferous laterites during preheating and reduction with carbon monoxide, *J. Therm. Anal. Calorim.*, 100(2010), No. 1, p. 133.

[16] T. Watanabe, S. Ono, H. Arai, and T. Matsumori, Direct reduction of garnierite ore for production of ferro-nickel with a rotary kiln at Nippon Yakin Kogyo Co., Ltd., Oheyama Works, *Int. J. Miner. Process.*, 19(1987), No. 1-4, p. 173.

[17] T. Matsumori, T. Ishizuka, and T. Matsuda, An economical smelting method of ferro-nickel as raw material of stainless steel, *Metall. Rev. MMIJ*, 13(1996), No. 1, p. 144.

[18] B.Z. Ma, P. Xing, W.J Yang, C.Y Wang, Y.Q Chen, and H. Wang, Solid-state metalized reduction of magnesium-rich low-nickel oxide ores using coal as the reductant based on thermodynamic analysis, *Metall. Mater. Trans. B*, 48(2017), No. 4, p. 2037.

[19] M. Jiang, T.C. Sun, Z.G. Liu, J. Kou, N. Liu, and S.Y. Zhang, Mechanism of sodium sulfate in promoting selective reduction of nickel laterite ore during reduction roasting process, *Int. J. Miner. Process.*, 123(2013), p. 32.

[20] M. Valix and W.H. Cheung, Effect of sulfur on the mineral phases of laterite ores at high temperature reduction, *Miner. Eng.*, 15(2002), No. 7, p. 523.

[21] W. Liang, H. Wang, J.G. Fu, and Z.X. He, High recovery of ferro-nickel from low grade nickel laterite ore, *J. Cent. South Univ.*, 42(2011), No. 8, p. 2173.

[22] C.C. Lin, Z.J. Liang, H.D. Hua, M. Rui, and J.G. Shao, Enrichment of nickel and iron from nickel laterite ore/coal composite pellets by deep reduction and magnetic separation, *J. Univ. Sci. Technol. Beijing*, 33(2011), No. 3, p. 270.

[23] F.M. Zhang, Progress of rotary hearth furnace direct reduction technology, [in] *5th International Conference on Science and Technology of Ironmaking*, Shanghai, 2009, p. 1347.

[24] Y.Y. Zhang, Y.H. Qi, Z.S. Zou, and Y.G. Li, Development prospect of rotary hearth furnace process in China, *Adv. Mater. Res.*, 746(2013), p. 533.